中國航空太空學會學刊第三十卷第四期第 309-319 頁（民國八十七年）
Transactions of the Aeronautical and Astronautical Society of the Republic of China, Vol.30, No.4, pp.309-319 (1998)

Flow Calculations on Moving and Sliding Grids

Tony W. H. Sheu, C. C. Fang, S. K. Wang, Y. H. Chen

Department of Naval Architecture and Ocean Engineering,
National Taiwan University
73 Chou-Shan Rd. Taipei, Taiwan, Republic of China.

Abstract

We consider in this paper several flow problems which are featured by having time-varying physical domains. The flow equations under investigation are Navier-Stokes equations for the incompressible fluid flow and the Euler equations for the highly compressible flow. The physical domain which varies with time adds additional complexities to the analysis of nonlinear partial differential equations which govern the fluid flows of the present interest. Depending on the nature of the time-varying physical domain, we extend flow analysis codes developed on fixed grids to moving and sliding grids so as to facilitate the analysis. As a first step in developing analysis codes to simulate the incompressible and compressible fluid flows in an arbitrarily configured domain, we consider some problems amenable to analytic solution to verify the ideas adopted and the code developed here. This is followed by investigating some geometrically complex problems of industrial importance.

Keywords: Navier-Stokes equations, Euler equations, moving grids, sliding grids.

在移動及滑動網格上之流體計算

許文翰、方昭清、王識貴、陳彥豪

國立台灣大學造船及海洋工程系(所)

摘要

本文考慮數個隨時間物理域可改變的流體力學問題。所分析的方程式爲不可壓縮之 Navier-Stokes 方程式及可壓縮之 Euler 方程式。由於物理空間的可變動性，使得分析更形複雜。依物理空間改變之特性，吾人將執行分析於移動及滑動的之網格上以利分析的進行。首先，吾人考慮具實解的問題，以便驗證程式之正確性。接著，吾人亦分析工業應用上有重要性之複雜幾何外型之問題。

關鍵字：那維爾－史多克方程式、歐意耳方程式、移動網格、滑動網格

1.Introduction

With the advent of faster computers with larger core memories and ever-improving computational techniques, computer simulation nowadays is playing an increasingly prominent role in large-scale industrial flow modelings or in configurations which are difficult to measure data in experiments. With this in mind, in the last decade we have developed finite volume and finite element codes, with success, to simulate incompressible Navier-Stokes equations and Euler equations, respectively. The approaches of which full

details can be found in [1-3] enable us to perform a detailed examination of the flow. Current efforts are directed toward the full use of the advantageous attributes of the computational fluid dynamics by extending the afore-mentioned codes formulated within the fixed grid context to their moving counterpart. While it is more elaborate and demanding than models implemented on fixed grids, the numerical simulation of flow problems on moving grids offers significant advantages and greatly extends the application scope.

Several numerical solutions to problems with moving boundaries have been reported. Among which, working equations formulated on moving coordinates and moving grids are often referred to. In the first class of methods for computing flows in a domain with arbitrarily moving boundaries, it is demanded that the field equations be formulated in general moving coordinates. The formulation of equations can be derived under the concept of Lie derivative [4]. This concept has been applied with success to compute flow fields around moving bodies by Ogawa and Ishiguro [5]. In their approach the computational coordinates fixed to the body move in space.

Another class of methods devised to achieve the same goal is to formulate field equations on moving grids. While the formulation on moving grids has enjoyed generality and, thus, has wider application scope, field equations which express physical conservation laws are constrained by the surface conservation law (SCL) and the volume conservation law (VCL). SCL was first pointed out by Trulio and Trigger [6] who dictated that cell volumes be closed by its surface while VCL demanded that the volumetric increment of a moving cell must be equal to the sum of the changes along the surface that encloses the volume. The necessity of incorporating this constraint condition into the formulation was not recognized until it was reiterated by Thomas and Lombard [7]. Later Demirdzic [8] and Warsi [9] also recognized the SCL as the fundamental constraint condition which should be solved together with the other conservation equations. Thomas and Lombard generalized these two laws in their pioneer work [7]. They called it the geometric conservation laws (GCL), establishing the conservative relations of the surfaces and volumes of the control cells. A flow simulation that does not satisfy the GCL, which governs the spatial volume element under an arbitrary mapping, produces errors and, thus, affects the solutions in two ways [10]. The numerical violation of the SCL leads to an erroneous representation of the convective velocities. In the case when the GCL is not solved simultaneously with other conservations, errors thus produced are represented as extra sources or sinks and are added to the physical conservation equations. Some representative papers are useful for the readers' reference [11-17].

More recently, an analysis which features its formulation on sliding grids has been proposed as another alternative to numerical simulation of problems with time-dependent grids [18-19]. The motivation behind the application of grids to flow analysis comes from the idea that has been frequently used in the area of solid mechanics. We will exploit this idea to problems which involve a rotating device in a restrictive physical domain.

The present paper is organized as follows. In Section 2, working equations for incompressible Navier-Stokes and compressible inviscid Euler equations are presented. Section 3 concentrates on moving grids for both flows while on sliding grids simply for the incompressible viscous fluid flows. Section 4 will detail methods by which finite element and finite volume solutions can be accurately predicted. This paper is followed by the description of the problems which are chosen to validate the methods proposed here. In Section 5, results are presented without paying too much attention on the discussion of results. In Section 6, we make concluding remarks.

2.Mathematical equations

We consider in this paper two flows of different characters. The first problem concerns the incompressible Navier-Stokes equations which are formulated on moving or on sliding grids. For completeness, we also consider compressible Euler equations, which govern the gas dynamics in two dimensions and are expressed on moving grids.

2.1 Incompressible Navier-Stokes equations

For simplicity, we will restrict our attention to the analysis of two-dimensional viscous incompressible flow. The nature of this flow is governed by the continuity equation and the Navier-Stokes equations given as follow:

$$u_x + v_y = 0\,, \tag{1}$$

$$u_t + uu_x + vu_y = -p_x + \mu(u_{xx} + u_{yy})\,, \tag{2}$$

$$v_t + uv_x + vv_y = -p_y + \mu(v_{xx} + v_{yy})\,. \tag{3}$$

In the above equations, we denote by p and u, v the pressure and velocity components, respectively. For simplicity, the kinematic viscosity of the fluid is considered uniform. Starting with the implementation of a divergence-free initial velocity vector, we seek a solution of (1-3) subject to proper boundary conditions.

2.2 Compressible Euler equations

Unlike the working equations given in (1-3) which

are cast in the primitive-variable form, the equations which are appropriate to describe inviscid and highly compressible gas dynamics are formulated in the strong conservation law form

$$\frac{\partial U}{\partial t}+\frac{\partial F}{\partial x}+\frac{\partial G}{\partial y}=\frac{\partial U}{\partial t}+A\frac{\partial U}{\partial x}+B\frac{\partial U}{\partial y}=0, \qquad (4)$$

where

$$U=[\rho,\rho u,\rho v,\rho e]^T, \qquad (5)$$

$$F=[\rho u,\rho u^2+p,\rho uv,u(p+\rho e)]^T, \qquad (6)$$

$$G=[\rho v,\rho uv,\rho v^2+p,v(p+\rho e)]^T, \qquad (7)$$

$$A=\begin{bmatrix} 0., & 1., & 0., & 0. \\ \frac{\gamma-1}{2}a^2-u^2, & (3-\gamma)u, & -(\gamma-1)v, & (\gamma-1) \\ -uv, & v, & u, & 0. \\ (\gamma-1)ua^2-\gamma ue, & \gamma e-\frac{1}{2}(\gamma-1)(a^2+2u^2), & -(\gamma-1)uv, & \gamma u \end{bmatrix} \qquad (8)$$

$$B=\begin{bmatrix} 0., & 0., & 1., & 0. \\ -uv, & v, & u, & 0. \\ \frac{\gamma-1}{2}a^2-v^2, & -(\gamma-1)u, & (3-\gamma)v, & (\gamma-1) \\ (\gamma-1)va^2-\gamma ve, & -(\gamma-1)uv, & \gamma e-\frac{1}{2}(\gamma-1)(a^2+2v^2), & \gamma v \end{bmatrix} \qquad (9)$$

In the above equations, ρ is denoted as the density, p the pressure, u, v, the velocity component along x and y direction respectively. e is the specific total energy, γ is the specific heat ratio and a is velocity defined by $a=(u^2+v^2)^{1/2}$. For the sake of closure, the equation of state for ideal gas is considered in the present study: $p=(\gamma-1)\rho(e-\frac{1}{2}u^2-\frac{1}{2}v^2)$. The main reason of representing working equations in conservation law form is that such a formulation permits the simulation of physical shocks and contact discontinuities in the flow interior.

3.Flow analyses on time-dependent physical domain

As alluded to earlier, we carry out flow analyses on moving and sliding grids. We begin by presenting some fundamentals for the methods adopted here.

3.1 Flow calculations on moving grids

The basis for an analysis formulated on moving grids is as follows. For a field variable in a moving grid system, the change of ϕ with time takes as the sum of the change due to moving grids and the change due to the field variable itself which varies with time. The above physical interpretation can be mathematically realized through the following identity equation.

$$\left.\frac{\partial\phi}{\partial t}\right|_{(\xi,\eta)}=\left.\frac{\partial\phi}{\partial t}\right|_{(x,y)}+(u_g,v_g)\cdot\nabla\phi \qquad (10)$$

In the above equation, (ξ,η) and (x,y) denote moving and fixed coordinates. Equation (10), which formulates the core of the present analysis, introduces grid velocities u_g, v_g into the flow formulation conducted on a time-varying domain:

$$u_g=\left.\frac{\partial x}{\partial t}\right|_{(\xi,\eta)} \qquad (11)$$

$$v_g=\left.\frac{\partial y}{\partial t}\right|_{(\xi,\eta)} \qquad (12)$$

Upon substituting equation (10) for a representative field variable to the momentum equations formulated on fixed grids, equations (2-3) cast on moving grids become

$$u_t+(u-u_g)u_x+(v-v_g)u_y=-p_x+\mu(u_{xx}+u_{yy}) \qquad (13)$$

$$v_t+(u-u_g)v_x+(v-v_g)v_y=-p_y+\mu(v_{xx}+v_{yy}) \qquad (14)$$

What is remarkable is that these equations bear close resemblance to their counterpart equations cast in fixed grids. A direct consequence of this resemblance is that the numerical solution of equations (13-14) requires no additional consideration other than that paid to the discretization of equations (2-3). The most difficult task is with the geometrical conservation law which has a close relevance to the grid velocities shown in equations (13-14). These two equations and equation (1), which is invariant in moving grids, constitute the core of the analysis for simulating problems where part of the surface bounding the flow region moves in time.

3.2 Flow calculations on sliding grids

For the description of analysis on sliding grids, we consider Navier-Stokes equations cast in cylindrical coordinates (r,θ,z):

$$\frac{1}{r}\frac{\partial(rv_r)}{\partial r}+\frac{1}{r}\frac{\partial v_\theta}{\partial\theta}=0 \qquad (15)$$

$$\frac{\partial v_r}{\partial t}+\frac{1}{r}\frac{\partial}{\partial r}(rv_r v_r)+\frac{1}{r}\frac{\partial}{\partial \theta}(v_r, v_\theta)$$
$$=\frac{1}{r}\frac{\partial}{\partial r}(\nu r\frac{\partial v_r}{\partial r})+\frac{1}{r}\frac{\partial}{\partial \theta}\left(\frac{\nu}{r}\frac{\partial v_r}{\partial \theta}\right)+\frac{v_\theta^2}{r}-\frac{2\nu}{r^2}\frac{\partial v_\theta}{\partial \theta}-\frac{\nu v_r}{r^2}-\frac{\partial p}{\partial r} \quad (16)$$

$$\frac{\partial v_\theta}{\partial t}+\frac{1}{r}\frac{\partial}{\partial r}(rv_r v_\theta)+\frac{1}{r}\frac{\partial}{\partial \theta}(v_\theta, v_\theta)$$
$$=\frac{1}{r}\frac{\partial}{\partial r}(\nu r\frac{\partial v_\theta}{\partial r})+\frac{1}{r}\frac{\partial}{\partial \theta}\left(\frac{\nu}{r}\frac{\partial v_\theta}{\partial \theta}\right)-\frac{v_r v_\theta}{r}+\frac{2\nu}{r^2}\frac{\partial v_r}{\partial \theta}-\frac{\nu v_\theta}{r^2}-\frac{1}{r}\frac{\partial p}{\partial \theta} \quad (17)$$

The analysis begins with the change of independent variables in between fixed coordinates (r,θ,z,t) and rotating coordinates $(r'=r,\theta'=\theta-wt,z'=z,t'=t)$. The rotation frequency is denoted as w. As a result of this transformation, the relations between velocity components v_r and v_θ and their corresponding velocity components read as $w_r=v_r$ and $w_\theta=v_\theta-wt$. Application of the chain rule leads to the working equations in rotating coordinates

$$\frac{\partial \phi}{\partial t}+\frac{1}{R}\frac{\partial}{\partial R}(RV\phi)+\frac{1}{R}\frac{\partial}{\partial \theta}(U\phi)=\frac{1}{R}\frac{\partial}{\partial R}(\Gamma R\frac{\partial \phi}{\partial R})+\frac{1}{R}\frac{\partial}{\partial \theta}(\frac{\Gamma}{R}\frac{\partial \phi}{\partial \theta})+S_\phi \quad (18)$$

where

	ϕ	R	θ	U	V	Γ
continuity eq.	1	r'	θ'	ω_θ	ω_r	ν
r' momentum eq.	ω_r	r'	θ'	ω_θ	ω_r	ν
θ' momentum eq.	ω_r	r'	θ'	ω_θ	ω_r	ν

	S_ϕ
continuity eq.	0
r' momentum eq.	$\frac{(\omega_\theta+\omega r')^2}{r'}-\frac{2\nu}{r'^2}\frac{\partial}{\partial \theta'}(\omega_\theta+\omega r')$ $-\frac{\nu\omega_r}{r'^2}-\frac{\partial p}{\partial r'}$
θ' momentum eq.	$-\frac{\omega_r(\omega_\theta+\omega r')}{r'}+\frac{2\nu}{r'^2}\frac{\partial \omega_r}{\partial \theta'}$ $-\frac{\nu\omega_\theta+\omega r'}{r'^2}+\frac{\nu\omega}{r'}-2\omega\omega_r$ $-\omega r'\frac{\partial \omega_r}{\partial r'}-\omega\frac{\partial \omega_\theta}{\partial \theta'}$ $-\frac{1}{r'}\frac{\partial p}{\partial \theta'}$

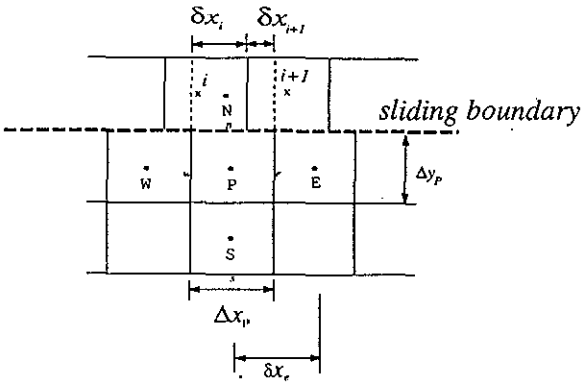

Figure 1: An illustration of two layers of grids which slide each other.

Referring to Fig.1, two layers of grids slide to each other. The main idea behind the analysis formulated on sliding grids is that flux retains conservation across the sliding boundary. With this underlying idea in mind, it is a simple matter of extending the analysis scope to sliding grids by rewriting v_r, v_θ and at the grid point 'N' to achieve the flux conservation. The resulting velocities are obtained as:

$$v_{rN}^*=\frac{v_{rN_{i+1}}\cdot\delta x_{i+1}+v_{rN_i}\cdot\delta x_i}{\Delta X_P} \quad (19)$$

$$v_{\theta N}^*=\frac{v_{\theta N_{i+1}}\cdot\delta x_{i+1}+v_{\theta N_i}\cdot\delta x_i}{\Delta X_P} \quad (20)$$

$$P_N^*=\frac{P_{N_{i+1}}\cdot\delta x_{i+1}+P_{N_i}\cdot\delta x_i}{\Delta X_P} \quad (21)$$

4.Discretization methods for working equations formulated on moving and sliding grids

Having derived the working equations on moving and sliding grids, we are to solve for dependent variables from them. Three analysis codes have been developed from scratch in the last decade. One was developed on the basis of finite volume method for analyzing three-dimensional Navier-Stokes equations. The other two are finite element codes developed for analyzing high-speed gas dynamics in two dimensions and for simulating three-dimensional Navier-Stokes equations, respectively. Due to space limitation, these codes are not detailed here.

4.1 Petrov-Galerkin monotone finite element model for incompressible flow simulation

There have been quite a few methods which can be applied with greater success to analyze Navier-Stokes

equations. We lay emphasis on the mixed formulation to ensure the satisfaction of divergence free character of the velocity vector which serves as a constraint on the motion of incompressible fluid flow. For the sake of presentation of the method, we will herein restrict ourselves to the two-dimensional analysis to enlighten the essential features embodied in the proposed method.

In what follows, we applied the method of weighted residuals to obtain the weak statement of the working equations. For retaining a smooth pressure solution, choice of finite elements warrants a consideration. The guideline is that the element in use must accommodate the LBB stability condition [20-21]. In the approximation of flux derivatives, the obstacle to giving a satisfactory scheme is attributed to convective terms which involve first derivative terms. For correctly accounting for the real physics in multiple dimensions, the downwind coefficients should be considered less significant than the upwind coefficients. Furthermore, the downwind coefficients should be negligibly small in comparison with those at the upwind nodes in the convective dominance case. For providing a upwinding effect to the formulation, the test space selected for use requires that test space be different from the basis space to enhance the stability of the discrete system. It is also desired to introduce the streamline operator into the formulation when constructing the test space. A direct benefit is that much of the false diffusion errors can be reduced in the simulation of multi-dimensional fluid flow where convective effect prevails.

The sole use of upwinding treatment, however, can not guarantee the solutions to be entirely monotonic. It may lead to a solution of unstable nature in the vicinity of sharp layers. Consequently, it has been a considerable impetus towards developing a genuine multi-dimensional monotone method for the transport equation. As inspired by the findings of Ahue's and Telias [22], we construct finite element stiffness matrix which falls into an M-matrix category [23-24]. To this end, we incorporate an exponential additive to the test function. It leads to

$$B_i(\xi,\eta)=\left[e\left(-\frac{\alpha u h_x}{2\nu}(\xi-\xi_i)\right)_e\left(-\frac{\beta v h_y}{2\nu}(\eta-\eta_i)\right)-1\right]M_i(\xi,\eta) \tag{22}$$

where h_x and h_y are grid sizes. It is emphasized that α and β are local parameters designed for providing a better solution accuracy. Substitution of the above test and basis functions to the weighted residuals statement, it yields a system of algebraic equations. One can refer to reference [3] for additional details.

4.2 Taylor-Galerkin finite element model with FCT filtering capability

Finite element method has ostensible advantages of providing geometric flexibility, application versatility, and automatic implementation of boundary conditions of the Neumann type. Besides these advantages, finite element analysis has a theoretical foundation to prove the convergence of solutions. Thus, use of the finite element method in modeling high speed compressible flow with possible discontinuities is on the rise in the field of aeroacoustics and gas dynamics.

The key to solving the above hyperbolic system given in (4-9) is to introduce the characteristic features into the discretization of flux terms. There are many characteristic discretization schemes to choose from. Among them, the characteristic finite element method [25], the discontinuous Galerkin method [26], the discontinuity capturing SUPG method [27], and the FCT finite element method [28-29], are often referred to. Whether there exists one approach which outperforms the others is not yet completely trivial to us and is believed to be a subject of continuous investigation.

Following the essence of the Taylor Galerkin model [30], we expand the flux terms via Taylor series expansion and then replace the higher-order time derivatives with the spatial derivatives. Inclusion of these higher-order terms brings in the hyperbolic property and, thus, enhances scheme stability and improves also phase accuracy. Having approximated the time derivative terms, we proceed to discretizing the remaining differential equations which involve only spatial derivatives by applying the Galerkin weighted residuals model. While stability of the discrete hyperbolic system has been enhanced, the added artificial viscosity causes the accuracy to deteriorate. Very often, numerical spreading is too excessive to allow accurate prediction of the transport phenomenon. Thus, there is strong motivation to develop an accurate scheme while retaining good stability in regions containing high gradient profiles.

The monotone positivity-preserving scheme was first investigated by Boris and Book [31] who proposed the Flux-Corrected-Transport (FCT) solution algorithm. This algorithm was later generalized by Zalesak [32] and extended to multi-dimensional analyses. The idea behind this nonlinear flux correction method is to combine a high-order scheme with a low-order scheme so that the former scheme can be used in smooth regions and the monotonic low-order scheme is in the vicinity of discontinuities. Later, Erlebacher [33] and Parrot et al. [34] applied the FCT technique to finite element flow analysis. Motivated by the success of Löhner et al. [35], the flux corrected transport technique of Boris and Book [31] will be employed in conjunction with the Taylor-Galerkin finite element model to solve the hyperbolic

system. Full details of this finite element code is given in [2].

By employing the Reynolds transport theorem as Probert indicated in [34], we have the following expression which invokes the reference frame speed (u_x, v_y):

$$\frac{d}{dt}\int_\Omega UW d\Omega = \int_\Omega \frac{\partial}{\partial t}(UW)d\Omega + \int_\Omega \left\{ \frac{\partial}{\partial x}(uxUW) + \frac{\partial}{\partial y}(u_y UW) \right\} d\Omega \tag{23}$$

This equation enables us to derive $\int W \partial U / \partial t \, d\Omega$ as follows:

$$\begin{aligned} \int_\Omega W\frac{\partial U}{\partial t}d\Omega &\equiv \int_\Omega \frac{\partial}{\partial t}(UW)d\Omega - \int_\Omega U\frac{\partial W}{\partial t}d\Omega \\ &= \frac{d}{dt}\int_\Omega (UW)d\Omega - \int_\Omega U\frac{dW}{dt}d\Omega - \int_\Omega W\left\{ \frac{d}{\partial x}(u_x U) + \frac{\partial}{\partial y}(u_y U) \right\} d\Omega \end{aligned} \tag{24}$$

By definition, the reference frame velocity takes on the same value as the mesh velocity, yielding

$$\frac{dW}{dt} = 0 \tag{25}$$

The finite element equations on moving grids are thus derived as

$$M\delta U^n = CF^n + \tilde{C}G^n + S \tag{26}$$

where

$$M^{el} = \left[M_{rs}^{el} \right] \tag{27}$$

$$\begin{aligned} M_{rs}^{el} = \int_{el} \Bigg\{ & N_i N_j - \frac{1}{2}\alpha\Delta t\left(\frac{\partial N_i}{\partial x}A + \frac{\partial N_i}{\partial y}B \right) N_j \\ & + \frac{1}{6}\gamma\Delta t^2 \left[\frac{\partial N_i}{\partial x}\left(A^2\frac{\partial N_j}{\partial x} + AB\frac{\partial N_j}{\partial y} \right) + \right. \\ & \left. + \frac{\partial N_j}{\partial y}\left(BA\frac{\partial N_j}{\partial x} + B^2\frac{\partial N_j}{\partial y} \right) \right] \Bigg\} d\Omega^{el} \\ & - \int \Bigg\{ -\frac{1}{2}\alpha\Delta t N_i (n_x A + n_y B) N_j \\ & + \frac{1}{6}\gamma\Delta t^2 N_i \Bigg[n_x \left(A^2\frac{\partial N_j}{\partial x} + AB\frac{\partial N_j}{\partial y} \right) \\ & + n_y \left(BA\frac{\partial N_j}{\partial x} + B^2\frac{\partial N_j}{\partial y} \right) \Bigg] \Bigg\} d\Gamma \end{aligned} \tag{28}$$

$$C^{el} = \left[C_{rs}^{el} \right] \tag{29}$$

$$\begin{aligned} C_{rs}^{el} = & \int_{\Omega^{el}} \frac{\partial N_i}{\partial x} \Bigg[\Delta t N_j - \frac{1}{2}\beta\Delta t^2 \left(A\frac{\partial N_j}{\partial x} + B\frac{\partial N_j}{\partial y} \right) \\ & + \frac{1}{6}\mu\Delta t^3 \left(A^2\frac{\partial^2 N_j}{\partial x^2} + AB\frac{\partial^2 N_j}{\partial x\partial y} \right. \\ & \left. + BA\frac{\partial^3 N_j}{\partial x\partial y} + B^2\frac{\partial^2 N_j}{\partial y^2} \right) \Bigg] d\Omega^{el} \\ & - \int n_x N_i \Bigg[\Delta t N_j - \frac{1}{2}\beta\Delta t^2 \left(A\frac{\partial N_j}{\partial x} + B\frac{\partial N_j}{\partial y} \right) \\ & + \frac{1}{6}\mu\Delta t^3 \left(A^2\frac{\partial^2 N_j}{\partial x^2} + AB\frac{\partial^2 N_j}{\partial x\partial y} \right. \\ & \left. + BA\frac{\partial^2 N_j}{\partial x\partial y} + B^2\frac{\partial^2 N_j}{\partial y^2} \right) \Bigg] d\Gamma \end{aligned} \tag{30}$$

$$\tilde{C}^{el} = \left[\tilde{C}_{rs}^{el} \right] \tag{31}$$

$$\begin{aligned} \tilde{C}_{rs}^{el} = & \int_{\Omega^{el}} \frac{\partial N_i}{\partial y} \Bigg[\Delta t N_j - \frac{1}{2}\beta\Delta t^2 \left(A\frac{\partial N_j}{\partial x} + B\frac{\partial N_j}{\partial y} \right) \\ & + \frac{1}{6}\mu\Delta t^3 \left(A^2\frac{\partial^2 N_j}{\partial x^2} + AB\frac{\partial^2 N_j}{\partial x\partial y} \right. \\ & \left. + BA\frac{\partial^3 N_j}{\partial x\partial y} + B^2\frac{\partial^2 N_j}{\partial y^2} \right) \Bigg] d\Omega^{el} \\ & - \int n_y N_i \Bigg[\Delta t N_j - \frac{1}{2}\beta\Delta t^2 \left(A\frac{\partial N_j}{\partial x} + B\frac{\partial N_j}{\partial y} \right) \\ & + \frac{1}{6}\mu\Delta t^3 \left(A^2\frac{\partial^2 N_j}{\partial x^2} + AB\frac{\partial^2 N_j}{\partial x\partial y} \right. \\ & \left. + BA\frac{\partial^2 N_j}{\partial x\partial y} + B^2\frac{\partial^2 N_j}{\partial y^2} \right) \Bigg] d\Gamma \end{aligned} \tag{32}$$

$$\begin{aligned} S = & -\int_{\Omega^{el}} \left(\frac{\partial N_i}{\partial x}u_x U + \frac{\partial N_i}{\partial y}u_y U \right) \Delta t N_j d\Omega \\ & + \int N_i \left(n_x u_x U + n_y u_y U \right) \Delta t N_j d\Gamma \end{aligned} \tag{33}$$

4.3 Finite volume method for the incompressible fluid flow

In the past decade we have developed an analysis code for simulating incompressible Navier-Stokes equations based on the finite volume method. To simulate the realistic flow problems involving complex geometry, we performed the analysis on curvilinear coordinate system. In curvilinear coordinates, full transformation approach which features the use of contravariant velocities as working variables was considered. The transformed equations bear a close resemblance to the equations formulated on Cartesian coordinates. As a result, flux discretization schemes so far developed on Cartesian coordinates can be applied to discretize the transformed equations. For solving a large-scale problem, we have a preference for a segregated method. Velocities and pressure are solved iteratively though a repeated correction of the solution built in the SIMPLE solution algorithm.

Before proceeding into the result and discussion section, we summarize here the discretized equation in the following form:

$$a_P\phi_P = a_E\phi_E + a_W\phi_W + a_N\phi_N + a_S\phi_S + b \tag{34}$$

where

$$a_E = D_e A(|P_e|) + \max(-F_e, 0) \tag{35}$$

$$a_W = D_w A(|P_w|) + \max(-F_w, 0) \tag{36}$$

$$a_N = D_n A(|P_n|) + \max(-F_n, 0) \tag{37}$$

$$a_S = D_s A(|P_s|) + \max(-F_s, 0) \tag{38}$$

$$F_e = (\rho U)_e \Delta y \tag{39}$$

$$D_e = \frac{\Gamma_e \Delta y}{(\partial x)_e} \tag{40}$$

$$P_i = \frac{F_i}{D_i} \quad \text{where} \quad i = e, w, n, s \tag{41}$$

$$A(|P_i|) = \max(0, (1 - 0.1|P_i|)^5) \tag{42}$$

$$a_P^0 = \frac{\rho_P^0 \Delta x \Delta y}{\Delta t} \tag{43}$$

$$b = S_C \Delta x \Delta y + a_P^0 \phi_P^0 \tag{44}$$

$$a_P = a_E + a_W + a_N + a_S + a_P^0 - S_P \Delta x \Delta y \tag{45}$$

$$S_\phi = S_P \phi_P + S_C \tag{45}$$

5.Results and discussion

We will present in this paper several test examples to show the applicability of three investigated codes to simulate flows in time-evolving physical domain. Description of flow physics embedded in the domain is left for future study.

5.1 Flow in a rolling-piston-type rotary compressor

The rolling-piston-type rotary compressor has been widely used in the air-conditioner and refrigeration for quite some time. Numerical exploration into this problem is of practical importance to increase the compressor efficiency without at the cost of increasing the noise. The physical problem under investigation is configured in Fig.2. The main components of the rotary compressor comprise two circular cylinders. The smaller circle, whose axis of rotation is not configured co-axially with the larger one, rotates tangentially with respect to the larger circle in the sense that there exists a seeming contact point. It is this contact point and the up-and-down moving vane, which locates in between the inlet and outlet port of the compressor, divides the flow passage into two parts. Depending on the direction of the inner rotating disk, the suction chamber is the one in the downstream end of the rotary circle while the compression chamber is on the upstream counterpart. As the design requires, the inlet port is kept open and the working gas is issued into the suction chamber. The outlet port is always closed except at the time when a high-pressure medium is discharged out of the compressor. It is worthy to note that the vane which moves up and down is used to prevent the gap to occur in between two chambers. The radius of the larger circle is with the value of 1 while the smaller one has the radius value of 0.875. The width of the vane is taken as 0.1.

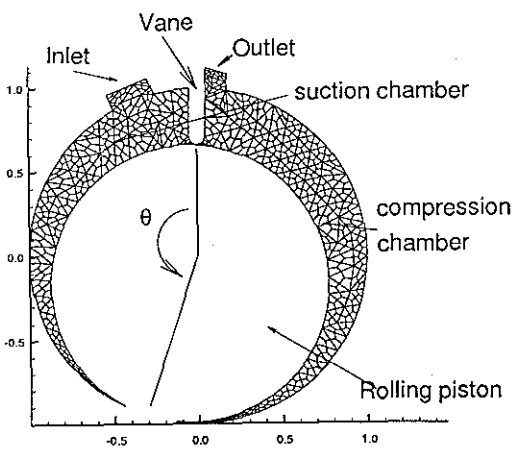

(a)

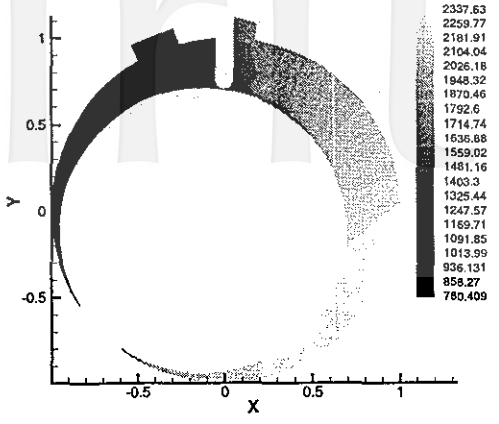

(b)

Figure 2: (a) The schematic of rolling-piston-type rotary compressor; (b) pressure contours computed at t = 0.325.

As an initial boundary-valued problem, initial conditions with ρ=1.4, p=1000, u=v=0 are prescribed to start the calculation. The rotary piston rotates counterclockwise with an angular speed $w = \pi$. The results which contain tremendous data have been presented in an animation fashion in the conference to provide readers a clear picture of the flow evolution.

5.2 Flow in a flexible vessel

The flexible vessel whose boundary is allowed to vary is shown schematically in Fig.3. This problem is chosen to demonstrate the validity of the Petrov-Galerkin finite element code formulated on moving grids. At the initial time t= 0, the velocity at the inlet, which is sufficiently upstream of the oscillating part of the vessel, is fully-developed in the originally straight vessel. As time develops, the flexible vessel of length 2 oscillates harmonically. At the opposite end which is located sufficiently downstream of the flexible section we prescribed there also a velocity profile of the zero-gradient type. The rest of the boundary condition is that of the no-slip type where velocity is prescribed with a value of zero. We have also presented an animated results in the conference. This facilitates us to gain physical details of the time-evolving vortical flow due to the oscillating motion of the flexible vessel.

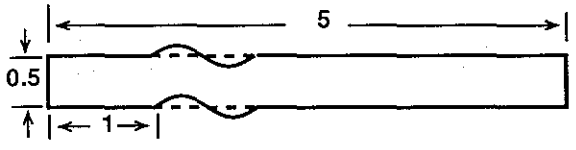

(a)

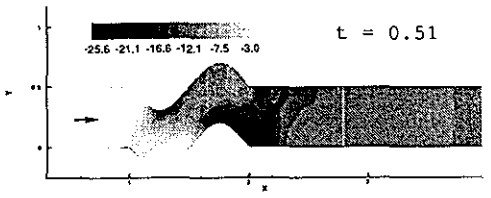

(b)

Figure 3: (a) The schematic of the flexible vessel containing a harmonic-moving section; (b) the pressure contours computed at t = 0.51.

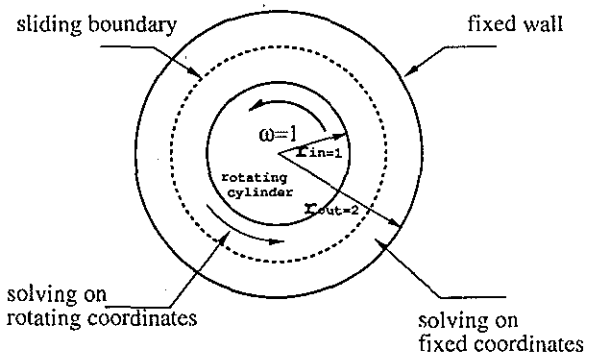

Figure 4: An illustration of the sliding grid configuration for the problem used to validate the code

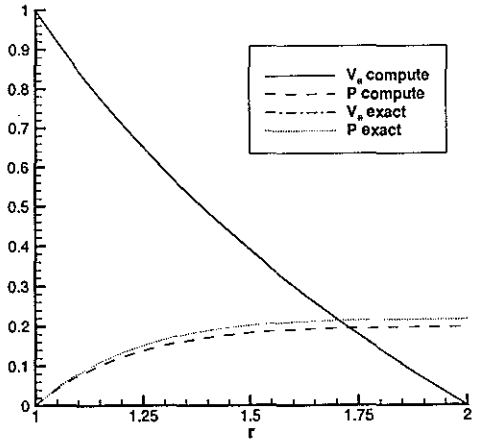

Figure 5: A comparison study of results computed from equations formulated on moving coordinates and sliding grids

5.3 Examples featured by having sliding grids

This paper is concluded by presenting results for problems which are most suited to be analyzed on sliding grids. The presentation of the results in this category begins with a co-axial two cylinder flow. As

Fig.4 shows, the inner cylinder rotates clockwise with a frequency of ω=1, while the outer cylinder is fixed. The problem can be either analyzed in rotating coordinates or in the grid system which contains two layers of grids. One of which slides with another, in between which there is an interface. Results obtained by solving the corresponding equations on their grids should provide the same solutions. In the light of above discussion, we can validate our code implemented on sliding grids. The comparison is shown in Fig.5, from which it is clear to see the close agreement between two sets of data.

We also present here some results of practical and military importance using the commercially available code, CFX, which also embodies the sliding grid capability. Test problems are known as the flow simulations in a mixing tank (Fig.6), cross-flow fan (Fig.7), and the submarine flow with rotating propellers (Fig.8). All these results are, as before, presented in the animation for the illustration purpose.

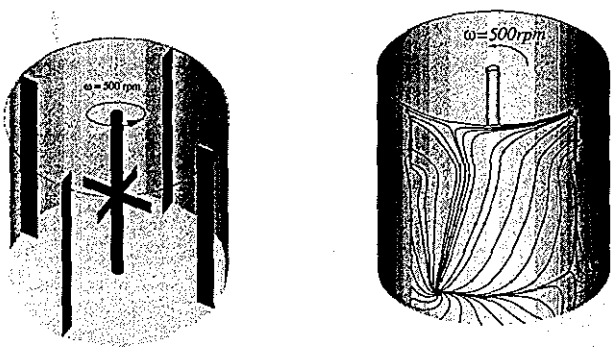

(a) (b)

Figure 6: (a) A Schematic of mixing tank with buffle plates; (b) the computed limiting streamlines on the tank side wall

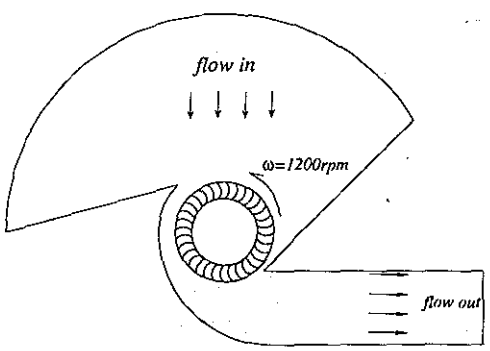

(a)

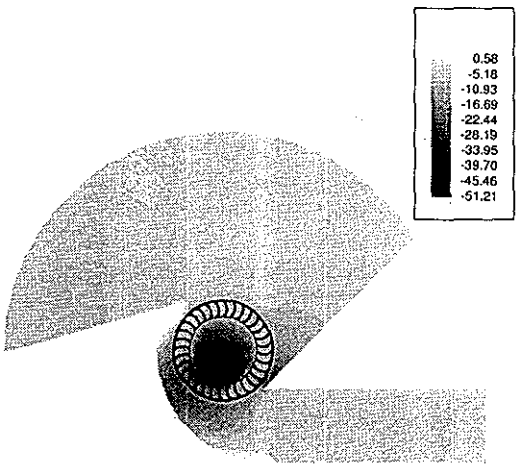

(b)

Figure 7: (a) A schematic of cross-flow fan; (b) the computed pressure contours

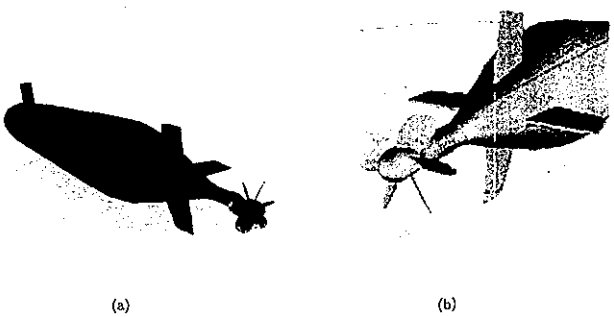

(a) (b)

Figure 8: (a) A schematic of submarine with propellers in rotation; (b) the particle tracerlines near the propeller.

6.Concluding remarks

This paper partly reports on three codes developed in the past decade. These finite volume and finite element codes have been originally developed on fixed grids to solve for incompressible Navier-Stokes equations in three dimensions and compressible Euler equations in two dimensions. The other focal point of this study is on the extending of these codes to moving and sliding grids. Test examples of academic as well practical importance have been attempted to address the usefulness of the sliding and moving grids to facilitate the analysis.

Acknowledgment

The authors would like to express their sincere

thanks to the Conference organizers who kindly invite us to present this paper in the 5th National Conference on Computational Fluid Dynamics. The authors would also like to acknowledge Dynatech Corporation, from which we are allowed to run CFX under their permission. Through technical consultation with their well-disciplined engineers, we can obtain the results to this point. Without doubt, the computer facilities offered by NCHC and Computer Center of the university I am teaching are also acknowledged. Finally, thanks also go to the financial support of NSC in the last decade that made the code development becomes possible.

References

[1] Tony W. H. Sheu, S. M. Lee, "A segregated solution algorithm for incompressible flows in general coordinates," Int. J. Numerical Methods in Fluids, Vol. 22, 1996, pp. 1-34.

[2] Tony W. H. Sheu, C. C. Fang, "A numerical study of nonlinear propagation of disturbances in two dimensions," J. of Computational Acoustics, Vol. 4 , No. 3, 1996, pp. 291-319.

[3] Tony W. H. Sheu, S. F. Tsai, M. M. T. Wang, "A Petrov-Galerkin formulation for incompressible flows at high Reynolds numbers," Int. J. Comput. Fluid Dyn., Vol. 5, 1995, pp. 213-230.

[4] J. A. Schouten, An Introduction to Tensor Analysis and its Geometrical Applications, 2nd edition, Springer-Verlag, Berlin, 1954.

[5] Satoru Ogawa and Tomiko Ishiguro, "A method for computing flow fields around moving bodies," J. Comput. Phys., Vol. 69, 1987, pp. 49-68.

[6] J. G. Trulio and K. R. Trigger, Numerical solution of the one-dimensional hydrodynamic equations in an arbitrary time-dependent coordinate system, Univ. of California Lawrence Radiation Lab. Report UCLR- 6522, 1961.

[7] P. D. Thomas and C. K. Lombard, "Geometric conservation law and its application to flow computations on moving grids," AIAA Journal, Vol. 17, 1979, pp. 1030-1037.

[8] Z. Demirdzic, A finite volume method of the Navier-Stokes equations in general nonstationary geometries, Ph.D. Thesis, University of London, 1982.

[9] Z. U. A. Warsi, "Conservation form of the Navier-Stokes equations in general unsteady coordinates," AIAA J., Vol. 19, 1981, pp. 240-242.

[10] M. Vinokur, "An analysis of finite-difference and finite-volume formulations of conservation laws," J. Comput. Phys., Vol. 81, 1989, pp. 1.

[11] J. A. Viecelly, "A computing method for incompressible flows bounded by moving walls," J. Comput. Phys., Vol. 8, 1979, pp. 119-143.

[12] S. K. Godunov and G. P. Prokopov, "The use of moving meshes on gas-dynamical computations," Zh. Vychisl, Mater. Mater. Fiz, Vol. 12 No.2, 1972, pp. 429-440.

[13] C. W. Hirt, A. A. Amsden and J. L. Cook, "An arbitrary Lagrangian-Eulerian computing method for all flow speeds," J. Comput. Phys., Vol. 14, 1974, pp. 227-253.

[14] D. Gosman and R. J. Johns, Development of a predictive tool for in-cylinder gas motion in engines, SAE paper 78 0315, 1978.

[15] M. E. Ralph and T. J. Pedley, "Flow in a channel with a moving indentation," J. Fluid Mech., Vol. 190, 1988, pp. 87-112.

[16] Z. Demirdzic and M. Peric, "Finite volume method for prediction of fluid flow in arbitrarily shaped domains with moving boundaries," Int. J. Numer. Meths. in Fluids, Vol. 10, 1990, pp. 771-790.

[17] H. Zhang, M. Reggio, J. Y. Trepanier, and R. Camarero, Computers Fluids, Vol. 22, No.1, 1993, pp. 9-23.

[18] AEA Technology, CFX 4.1 Flow solver User guide, U.K., 1995.

[19] X. M. Li and P. P. Ma, Three dimensional flow in an axially grooved rotor-stator configuration, Proceddings of the Ninth Int. Conf. Numerical Methods in Laminar and Turbulent Flow, Atlanta, C. Taylor and P. Durbetaki (eds.), vol. IX, Part 1, 1995, pp. 394-405.

[20] F. Brezzi, On the existence, "uniqueness and approximation of saddle point problems arising form Lagrangian multipliers," RAIRO, Anal. Num., Vol. 8 (R2), 1974, pp. 129-151.

[21] Babuska, "Error bounds for finite element methods." Numer. Math., Vol. 16, 1971, pp. 322-333.

[22] M. Ahue's and M. Telias, "Petrov-Galerkin scheme for the steady state convection-diffusion equation," Finite Elements in Water Resources, 1982, pp. 2/3-2/12.

[23] Theodor Meis, Ulrich Marcowitz, Numerical Solution of Partial Differential Equations, Applied Mathematical Science, Vol. 32, Springer-Verlag, 1980.

[24] Tsutomu Ikeda, "Maximal Principle in Finite Element Models for Convection-Diffusion Phenomena," Lecture Notes in Numerical and Applies Analysis, Vol. 4, North-Holland, 1983.

[25] K. W. Morton, "Generalized Galerkin methods for hyperbolic problems." Computer Methods in Applied Mechanics and Engineering, Vol. 52, 1985, pp. 847-871.

[26] P. Lesaint and P. A. Raviart, On a finite element method for solving the neutron transport problem. In C. de Boor (ed.), Mathematical Aspects of Finite Elements in Partial Differential Equations, Academic Press, 1974, pp. 89-123.

[27] T. J. R. Hughes, M. Mallet and A. Mizukami, "A new finite element formulation for computational

fluid dynamics: II. Beyond SUPG." Computer Methods in Applied Mechanics and Engineering, Vol 54, 1986, pp. 341-355.

[28] R. Löhner, K. Morgan and O. C. Zienkiewicz, "The solution of nonlinear system of hyperbolic equation by the finite element method." Int. J. Numer. Methods Fluids, Vol. 4, 1984, pp. 1043-1063.

[29] T. W. H. Sheu, C. C. Fang, S. H. Kuo and J. Y. Yang, "A high resolution capturing finite element method." Proc. of 5th International Symposium on Computational Fluid Dynamics, Tohoku University, Japan, H. Daiguji (eds.), {\bf 3}, 1993, pp. 103-108.

[30] J. Donea, "A Taylor-Galerkin method for convective transport problems." Int. J. for Numer. Meths. Engrg., Vol. 20, 1984, pp. 101-119.

[31] J. P. Boris and D. L. Book, "Flux-corrected transport, I SHASTA, a fluid transport algorithm that works." J. Comput. Phys., Vol. 11, 1973, pp. 38-69.

[32] S. T. Zalesak, "Fully multidimensional flux-corrected transport algorithm for fluids." J. Comput. Phys., Vol. 31, 1979, pp. 335-362.

[33] G. Erlebacher, Solution adaptive triangular meshes with application to simulation of plasma equilibrium. Ph. D Thesis, Columbia University, 1984.

[34] K. Parrot and M. A. Christie, Solution adaptive triangular meshes with application to the simulation of plasma equilibrium. In K. W. Morton and M. J. Baines (eds.), Numerical Methods for Fluid Dynamics, Oxford University, 1986, pp 609-620,.

[35] R. Löhner, K. Morgan, J. Peraire and M. Vahdati, "Finite element flux corrected transport (FEM-FCT) for the Euler and Navier-Stokes equations." Int. J. Numer. Meths. In Fluids, Vol. 7, 1987, pp. 1093-1109.

Paper presented at The 5th CONFERENCE ON COMPUTATIONAL FLUID DYNAMICS, Tao-Yuan, Taiwan, reviewed processed and recommended by Associate editor Dr. Dhng-Hsien Dai; accepted for publication NOV.1 1998